

ISOGOMETRIC ANALYSIS FOR DOMAINS WITH CORNERS

Q. XU^{*}, F. WANG[†], K.S. LAI[†] AND G. LIN[†]

^{*} Dalian University of Technology
School of Hydraulic Engineering, 116024 Dalian, China
xuqingdut@gmail.com

[†] Dalian University of Technology
School of Hydraulic Engineering, 116024 Dalian, China
wangfengdut@gmail.com

Key Words: *Isogeometric analysis, NURBS, Laplace equation, Corner.*

Abstract. Isogeometric analysis (IGA) based on the non-uniform rational B-spline (NURBS) basis functions provides an effective integration between computer aided geometry design (CAGD) and the finite element method (FEM). This method can effectively reduce the error of geometric discretization and significantly improve the computational accuracy. Moreover, it is very easy to construct higher-order smooth continuous NURBS basis functions. This paper extends IGA to solve the Laplace equation whose domain contains the reentrant corners. The physical field is constructed by the same NURBS basis functions as the representation of the geometric model. The governing equation is discretized using the standard Galerkin method. Repeated control points and multipatch are proposed for IGA whose domain contains the reentrant corners. For multipatch case, knot vectors and control points must coincide on the interface of different patches, even after refinement. C^0 -continuity across the patch interfaces can be maintained. Here we present several numerical examples to show that our method can approximate the singular solutions in domains with corners.

1 INTRODUCTION

The simplified domains of many engineering problems contain sharp edges and corners, and these often pose important challenges in numerical analyses. Typical examples are reentrant corners in fluid mechanics [1], crack tip problems in fracture mechanics [2,3]. In this paper, we adopt the isogeometric analysis (IGA) to solve the Laplace equation for domains with corners. IGA based on non-uniform rational B-splines (NURBS) has been proposed by Hughes.[4] The main feature of IGA is the ability to use the same NURBS basis functions for the geometry parameterization and the PDE solution space. This method could maintain the same exact representation of the computational domain geometry throughout the analysis process, including refinement. IGA shares several prominent features with the meshless method such as higher continuity of the field function, better convergence on a per-degree-of-freedom basis. For this method, there exist three versatile refinement procedures, which are the h -refinement of knot insertion, the p -refinement of order elevation, and the unique k -refinement. The refinement process is implemented easily, which does not need to

communicate with the original geometric model. This method has attracted rapidly growing research interests and wide applications. Now IGA has been successfully applied to various fields such as structure[5], fluids[6], electromagnetics[7-9]. Zhang[10] combined the scaled boundary finite element method with IGA. Simpson[11] applied the NURBS basis functions to BEM to solve linear elastostatic problems.

However, in almost all practical circumstances, it will be necessary to describe domains with multiple NURBS patches. For example, if different materials or physical models are to be used in different parts of the domain, it might simplify things to describe these subdomains by different patches. The tensor product of the parameter space of a patch makes it particularly suited for representing complex, multiply connected domain. C^0 -continuity across the patch interfaces is the most frequently used in multipatch isogeometric analysis up to now.

In this paper, IGA is extended to solve the Laplace equation implemented on multipatch conforming geometries. The multipatch geometry is formed using the patch splicing technique and C^0 -continuity across the patch interfaces could be maintained. This method has proved capable of approximating singular solutions with a good convergence rate. This paper is organized as follows. A brief overview on IGA is made in section 2. In section 3, we focus on isogeometric analysis to the Laplace equation. In section 4, we present two numerical examples which confirm the good performance of IGA.

2 A BRIEF OVERVIEW ON ISOGEOMETRIC ANALYSIS

2.1 B-splines and NURBS

A knot vector Ξ is a set of non-decreasing real numbers representing coordinates in the parametric space of the curve: $\Xi = \{\xi_1, \dots, \xi_{n+p+1}\}$, where $\xi_i \in \Xi$ is the i th knot, i is the knot index, $i = 1, 2, \dots, n+p+1$, p is the polynomial degree, and n is the number of basis functions which comprise the B-spline. The knot vector Ξ is said to be open if its first and last knots repeat $(p+1)$ times. Open knot vectors are standard in the CAD literature. With the given knot vector Ξ , the univariate B-spline basis functions can be constructed by the following recursive formula:

$$\left\{ \begin{array}{l} N_{i,0}(\xi) = \begin{cases} 1 & \text{if } \xi_i \leq \xi \leq \xi_{i+1} \\ 0 & \text{otherwise} \end{cases} \\ N_{i,p}(\xi) = \frac{\xi - \xi_i}{\xi_{i+p} - \xi_i} N_{i,p-1}(\xi) + \frac{\xi_{i+p+1} - \xi}{\xi_{i+p+1} - \xi_{i+1}} N_{i+1,p-1}(\xi), p \geq 1 \end{array} \right. \quad (1)$$

In Fig.1, an example consisting of $n=7$ quadratic B-spline basis functions is presented using the following knot vector $\Xi = \{0, 0, 0, 0.2, 0.4, 0.6, 0.8, 1, 1, 1\}$. Clearly the B-spline basis functions can be C^1 continuous and have non-interpolatory nature in the interior domain, while the basis functions formed by the open knot vector interpolate both end values.

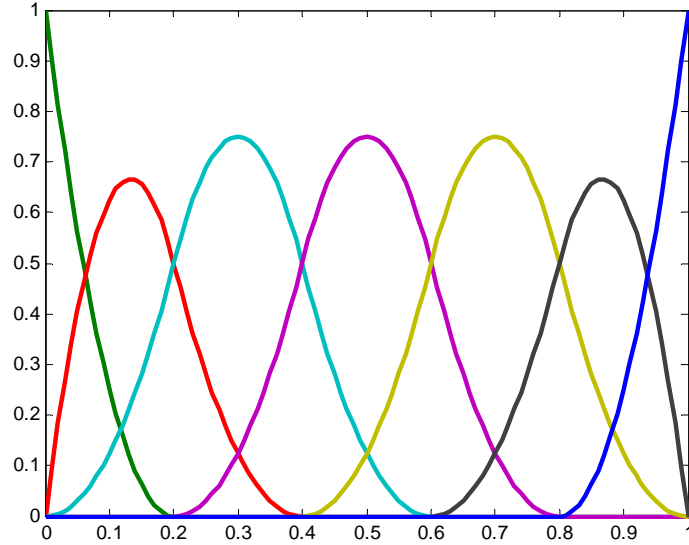


Figure 1: Quadratic B-spline basis functions

The NURBS basis function $R_{i,p}(\xi)$ can be built from B-spline basis function via rationalization, that is

$$R_{i,p}(\xi) = \frac{N_{i,p}(\xi)w_i}{\sum_{j=1}^n N_{j,p}(\xi)w_j} \quad (2)$$

If all the weights are equal, the NURBS basis functions degenerate to B-spline basis functions.

B-splines and NURBS allow to easily reproduce both FEM typical refinement strategy, namely, h -refinement and p -refinement, by means of knot insertion and degree elevation procedures, respectively. A third particularly effective option is also offered by the k -refinement, which consists of a high-regularity refinement strategy.

By using the NURBS basis functions, a curve can be formed as

$$C(\xi) = \sum_{i=1}^n R_{i,p}(\xi)P_i \quad (3)$$

where P_i are the coefficients of NURBS basis functions, which denote the control points.

2.2 The general framework of isogeometric analysis

IGA aims to achieve the numerical approximation to the solution of PDEs, which is also for FEM. In both approaches, the PDEs are numerically solved using the Galerkin procedure in which the solution of PDEs is sought in a finite-dimensional space with good approximation properties and the PDEs are written in their equivalent variational formulations.

Let us consider a two-dimensional case, where we assume that the physical domain $\Omega \subset \mathbb{R}^2$ is open, bounded and Lipschitz. Suppose now that such a domain is parameterized by a global geometry function

$$\mathbf{F}: \hat{\Omega} \rightarrow \Omega, \quad \mathbf{F}(\xi, \eta) = \begin{pmatrix} x \\ y \end{pmatrix} \quad (4)$$

where $\hat{\Omega}$ is the parametric domain (e.g., the unit square), and the value of the parameterization can be computed with the information given by the CAD software. The parameterization \mathbf{F} is assumed to be smooth with piecewise smooth inverse.

In IGA, the field variable $u(\mathbf{x})$ and the geometry are represented similarly to the isoparametric finite element method as follows:

$$\begin{cases} \mathbf{x} = \sum_{i=1}^n N_i(\xi) \mathbf{P}_i \\ u^h(\mathbf{x}) = \sum_{i=1}^n N_i(\xi) \mathbf{u}_i \end{cases} \quad (5)$$

where n represents the number of control points as well as the basis functions. $N_i(\xi)$ is the NURBS basis function, and \mathbf{u}_i is the control variable associated with the control point \mathbf{P}_i .

$$\mathbf{x} = (x, y), \quad \xi = (\xi, \eta).$$

3 DISCRETIZATION OF THE LAPLACE EQUATION AND NURBS MULTIPATCH CONFORMING GEOMETRIES

3.1 Discretization of the Laplace equation

The geometry domain discretization requires a knot vector for each parametric direction, $\xi = \{\xi_1, \xi_2, \dots, \xi_{n+p+1}\}$ and $\eta = \{\eta_1, \eta_2, \dots, \eta_{m+q+1}\}$. p and q are the degree of NURBS basis functions in two independent directions. Here we introduce the knot vector ξ' and η' without repetitions. The knot interval $[\xi_i^k, \xi_{i+1}^k] \times [\eta_j^k, \eta_{j+1}^k]$ is mapped into the element $Q^{i,j}$ on physical domain.

Considering the Laplace equation in the domain Ω bounded by $\partial\Omega$ can be written as

$$-\nabla^2 u = f \quad \text{in } \Omega \quad (6)$$

The boundary $\partial\Omega$ is split into two disjoint parts, $\partial\Omega = \Gamma_N \cup \Gamma_D$. The Dirichlet boundary conditions on Γ_D are:

$$u = 0 \quad \text{on } \Gamma_D \quad (7)$$

The Neumann boundary conditions on Γ_N are:

$$\frac{\partial u}{\partial \mathbf{n}} = 0 \quad \text{on } \Gamma_N \quad (8)$$

Where \mathbf{n} is the normal vector.

The Laplace equation in its variational formulation reads as: Find $u \in \mathbf{H}_{0,\Gamma_D}^1(\Omega)$, such that

$$\int_{\Omega} \nabla u \cdot \nabla v \, d\Omega = \int_{\Omega} f v \, d\Omega \quad \forall v \in \mathbf{H}_{0,\Gamma_D}^1(\Omega) \quad (9)$$

$\mathbf{H}_{0,\Gamma_D}^1(\Omega) = \{v \in \mathbf{H}^1(\Omega) : v = 0 \text{ on } \Gamma_D\}$ is the space of functions with vanishing trace on Γ_D .

The Galerkin procedure consists of approximating the infinite-dimensional space V by a finite-dimensional space V_h . The variational formulation of the discrete equation is: Find $u_h \in V_h$ such that

$$\int_{\Omega} \nabla u_h \cdot \nabla v_h \, d\Omega = \int_{\Omega} f v_h \, d\Omega \quad \forall v \in V_h \quad (10)$$

Upon inserting u_h into the weak form (10) and testing with $v_h = N_i$, one obtains the following linear system

$$\mathbf{K}u = \mathbf{b} \quad (11)$$

Where the global stiffness matrix and the global force vector assembled from the element stiffness matrices and the local force vectors are $\mathbf{K} = \sum_{i,j} \mathbf{K}_{ij}$ and $\mathbf{b} = \sum_{i,j} \mathbf{b}_{ij}$, respectively.

$$\mathbf{K}_{ij} = \int_{\xi_i^k}^{\xi_{i+1}^k} \int_{\eta_j^k}^{\eta_{j+1}^k} \mathbf{B}(\xi, \eta)^T \mathbf{B}(\xi, \eta) |J| \, d\xi \, d\eta \quad (12)$$

$$\mathbf{b}_{ij} = \int_{\xi_i^k}^{\xi_{i+1}^k} \int_{\eta_j^k}^{\eta_{j+1}^k} N(\xi, \eta)^T f |J| \, d\xi \, d\eta \quad (13)$$

Where $N(\xi, \eta)$ and $\mathbf{B}(\xi, \eta)$ are the NURBS shape functions and the gradient of NURBS shape functions of element $Q^{i,j}$.

$$N(\xi, \eta) = \{N_1(\xi, \eta) \quad N_2(\xi, \eta) \quad \dots \quad N_n(\xi, \eta)\} \quad (14)$$

$$\mathbf{B}(\xi, \eta) = \begin{bmatrix} \frac{\partial N_1(\xi, \eta)}{\partial \xi} & \frac{\partial N_2(\xi, \eta)}{\partial \xi} & \dots & \frac{\partial N_n(\xi, \eta)}{\partial \xi} \\ \frac{\partial N_1(\xi, \eta)}{\partial \eta} & \frac{\partial N_2(\xi, \eta)}{\partial \eta} & \dots & \frac{\partial N_n(\xi, \eta)}{\partial \eta} \end{bmatrix} \quad (15)$$

The integration interval in Eqs.(12) and (13) is the knot interval in parametric space of NURBS element $Q^{i,j}$, which varies from element to element.

3.2 NURBS multipatch conforming geometries

In order to analyze domains of complex topology with conventional isogeometric analysis, several tensor product pieces should be patched together before analysis procedures. Here we assume that the patches are compatible, in the sense that knot vectors and control points must coincide on the interface, even after refinement. Therefore, refinements of one patch can propagate from that patch to the next. In our specific case, the physical domain Ω is represented by n single patch Ω_i , $i=1,2,\dots,n$. Each patch Ω_i is defined by a parametrization of the form $\mathbf{F} \equiv \mathbf{F}_i : \hat{\Omega} \rightarrow \Omega_i$. If Ω_i and Ω_j are two patches with a common interface Γ_{ij} , and ℓ_i, ℓ_j are their respective meshes, then they must coincide on the interface, i.e., $\ell_i|_{\Gamma_{ij}} = \ell_j|_{\Gamma_{ij}}$, with the same knot multiplicities at $\mathbf{F}_i^{-1}(\Gamma_{ij})$ and $\mathbf{F}_j^{-1}(\Gamma_{ij})$. This yields a global C^0 parametrization of the domain Ω and also a C^0 tangential component for our discrete solutions. However, the continuity is retained at its maximum in the interior of each patch. A subscript f is used to denote the control points on the face where the patches meet, and a subscript n to denote the control points not on that face. We may write the control

points for patches Ω_i and Ω_j .

$$\mathbf{P}^1 = \begin{pmatrix} \mathbf{P}_n^1 \\ \mathbf{P}_f^1 \end{pmatrix} \quad \text{and} \quad \mathbf{P}^2 = \begin{pmatrix} \mathbf{P}_n^2 \\ \mathbf{P}_f^2 \end{pmatrix} \quad (16)$$

respectively, where

$$\mathbf{P}_f^2 = \mathbf{P}_f^1 \quad (17)$$

C^0 -continuity of the geometry is maintained by the relationship

$$\sum_{\Gamma_{ij}} N_i(\xi) \mathbf{u}_i = \sum_{\Gamma_{ij}} N_j(\xi) \mathbf{u}_j \quad (18)$$

4 NUMERICAL RESULTS

4.1 The curved L-shaped domain

The first test concerns with the computation of Laplace equation in a nonconvex geometry, that is a curved L-shaped domain. The geometry consists of two patches that match C^0 with continuity. Clearly, the coarsest mesh can be formed by only two elements to obtain the exact geometry. This is the clear advantage compared to finite element method. The corresponding mesh for the curved L-shaped domain is shown in Fig.2.

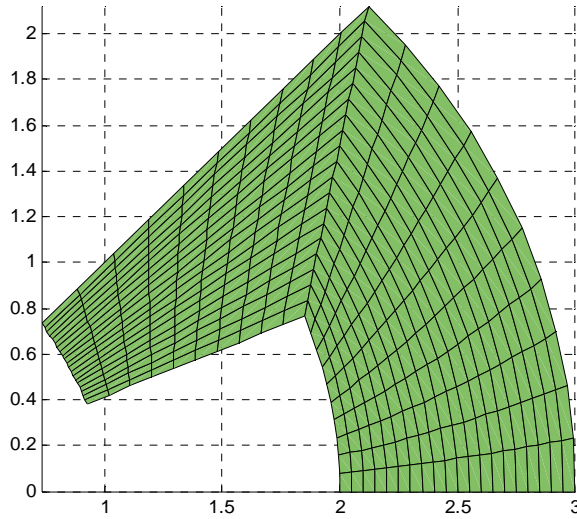


Figure 2: Mesh for the curved L-shaped domain

Fig.3 shows the numerical approximation and Fig.4 shows the distribution of the absolute error. This parameterization is globally C^2 -continuous and the degree is $p = 3$. In order to evaluate the error in the solutions, we use the following L_2 norm

$$\| \mathbf{u} - \mathbf{u}^h \|_{L_2(\Omega)} = \left(\int_{\Omega} (\mathbf{u} - \mathbf{u}^h)^2 d\Omega \right)^{1/2} \quad (19)$$

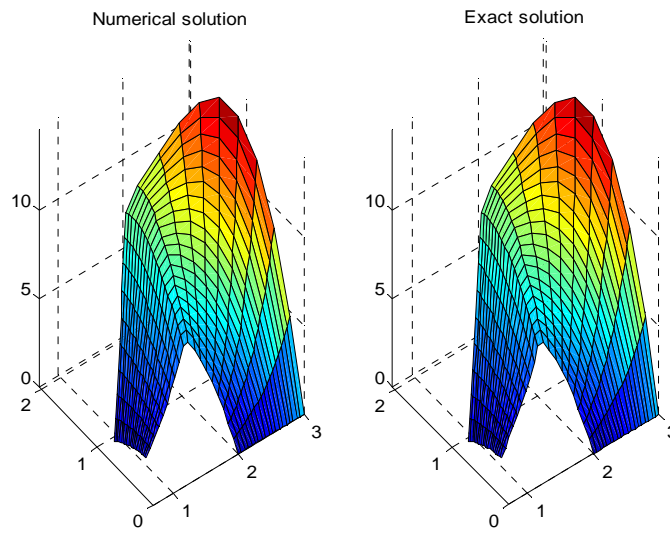


Figure 3: Numerical solution for 276 degrees of freedom

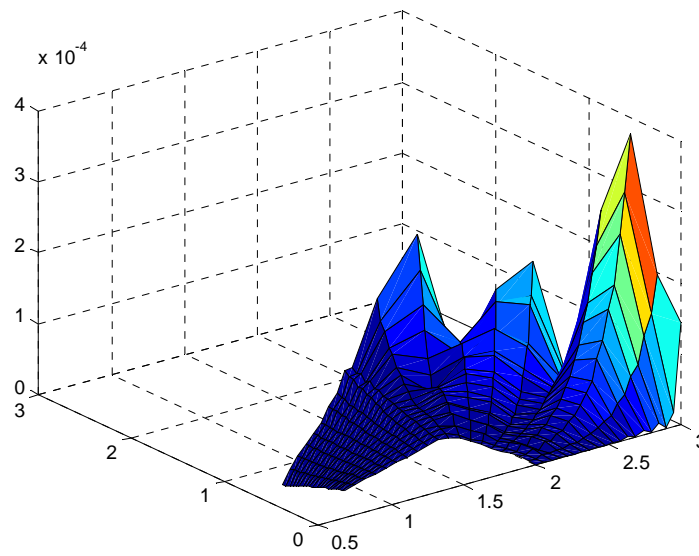


Figure 4: Absolute error for the numerical approximation solution

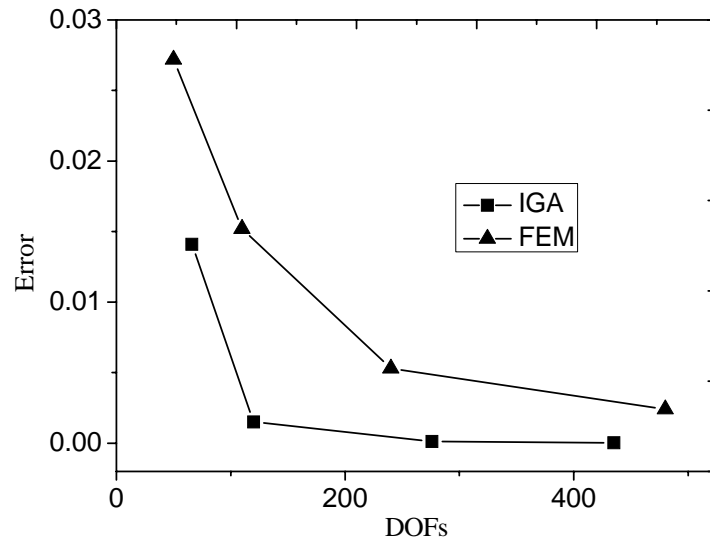


Figure 5: Convergence of the error for the solutions

4.2 Bifurcation

The bifurcation domain with regard to the computation of Laplace equation is considered in the second test. The geometry consists of four patches that match C^0 with continuity. The corresponding mesh for the bifurcation domain is shown in Fig.6. The L_2 norm is just 1.3770×10^{-4} . Fig.7 shows the contour plots of u .

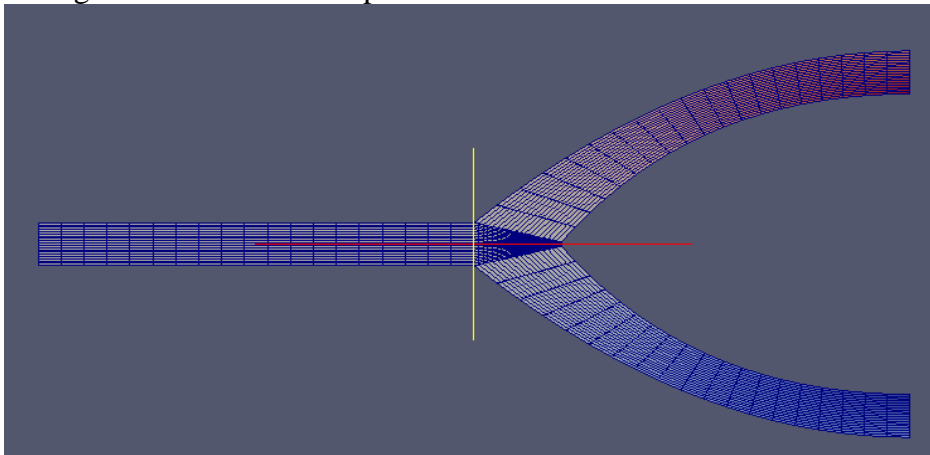


Figure 6: Mesh for the bifurcation domain

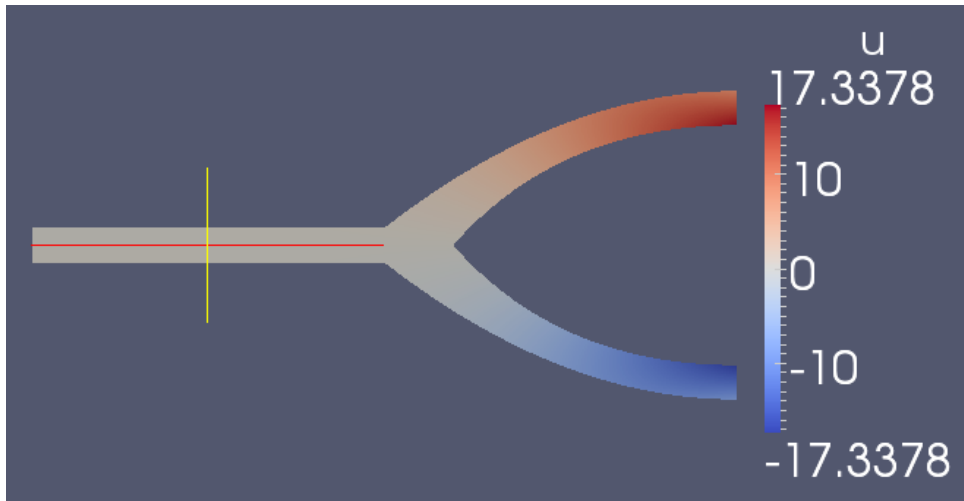


Figure 7: Contour plots of u

5 CONCLUSIONS

In this paper, IGA based on the multipatch conforming geometries has been applied to solve the Laplace equation for domains with corners. We have considered h -, p -, and k -refinement strategies, treatment of multipatch geometries. Comparing the results of IGA with those of FEM, the higher accuracy and faster convergence can be obtained. For the multipatch geometries, the control point and the control variable of the solution on a face should be in one-to-one correspondence with the control point and the control variable from the adjoining face. Combining the patch splicing with the patch removal is the key issue in the engineering application for IGA.

ACKNOWLEDGMENT

The authors acknowledge the GeoPDEs-Innovative compatible discretization techniques for Partial Differential Equations.

REFERENCES

- [1] Lesnic, D., Elliott, L. and Ingham D.B. Treatment of singularities in exterior fluid domains with corners using the boundary element method. *Comput. Fluids*. (1994) **23**:817-827.
- [2] Martinez, J. and Dominguez, J. On the use of quarter-point boundary elements for stress intensity factor computations. *Int. J. Numer. Meth. Eng.* (1984) **17**:1941-1950.
- [3] Aiza, M.P., Saez, A. and Dominguez, J. A singular element for three-dimensional fracture mechanics analysis. *Eng. Anal. Bound. Elem.* (1997) **20**:275-285.
- [4] Hughes, T.J.R., Cottrell, J.A. and Bazilevs, Y. Isogeometric analysis: CAD, finite elements, NURBS, exact geometry and mesh refinement. *Comput. Methods. Appl. Mech. Eng.* (2005) **194**: 4135-4195.
- [5] Cottrell, J.A., Reali, A., Bazilevs, Y. and Hughes, T.J.R. Isogeometric analysis of structural vibrations. *Comp. Meth. Appl. Mech. Eng.* (2006) **195**: 5257-5296.
- [6] Bazilevs, Y., Calo, V.M., Zhang, Y., and Hughes, T. J. R. Isogeometric fluid–structure

- interaction analysis with applications to arterial blood flow. *Comput. Mech.* (2006) **38**: 310-322.
- [7] Buffa, A., Sangalli, G., and Vázquez, R. Isogeometric analysis in electromagnetics: B-splines approximation. *Comp. Meth. Appl. Mech. Eng.* (2010) **199**: 1143-1152.
- [8] Vázquez, R. and Buffa, A. Isogeometric Analysis for Electromagnetic Problems. *IEEE. Trans. Magn.* (2010) **46**: 3305-3308.
- [9] Buffa, A., Sangalli, G., Rivas, J. and Vazquez, R. Isogeometric Discrete Differential Forms in Three Dimensions. *SIAM J. Numer. Anal.* (2011) **49**: 818-844.
- [10] Zhang, Y., Lin, G., and Hu, Z.Q. Isogeometric analysis based on scaled boundary finite element method. *IOP Conference Series: Materials Science and Engineering* (2010) **10**: 012237.
- [11] Simpson, R.N., Bordas., S.P.A., Trevelyan, J., and Rabczuk, T. A two-dimensional Isogeometric Boundary Element Method for elastostatic analysis. *Comp. Meth. Appl. Mech. Eng.* (2012) **209**: 87-100.
- [12] Piegl, L. and Tiller, W. *The NURBS book*. Springer Verlag, Vol. II, (1997).